Three-dimensional Location of Human Rectus Pulleys by Path Inflections in Secondary Gaze Positions

Robert A. Clark,[1,2] *Joel M. Miller,*[3] *and Joseph L. Demer*[1,4]

Purpose. Connective tissue pulleys serve as the functional mechanical origins of the extraocular muscles (EOMs). Anterior to these pulleys, EOM paths shift with gaze to follow the scleral insertions, whereas posterior EOM paths are stable in the orbit. Inflections in EOM paths produced by gaze shifts can be used to define the functional location of pulleys in three dimensions (3-D).

Methods. Contiguous magnetic resonance images in planes perpendicular to the orbital axis spanned the anteroposterior extents of 22 orbits of 11 normal adults with the eyes in central gaze, elevation, depression, abduction, and adduction. Mean EOM cross-sectional area centroids represented in a normalized, oculocentric coordinate system were plotted over the length of each EOM to determine paths. Path inflections were identified to define pulley locations in 3-D.

Results. All rectus EOM paths exhibited in secondary gaze positions distinct inflections 3 to 9 mm posterior to globe center, which were consistent across subjects. The globe center and the lateral rectus pulley translated systematically in the orbit with lateral gaze, whereas other pulleys remained stable relative to the orbit.

Conclusions. Distinct inflections in rectus EOM paths in secondary gaze positions confirm the existence of pulleys and define their locations in 3-D. The globe and lateral rectus pulley translate systematically with gaze position. The EOM pulleys may simplify neural control of eye movements by implementing a commutative ocular motor plant in which commands for 3-D eye velocity are effectively independent of eye position. (*Invest Ophthalmol Vis Sci.* 2000;41:3787–3797)

Recent reexamination of orbital histology has defined connective tissue sleeves enveloping the rectus extraocular muscles (EOMs) in the region of posterior Tenon's capsule posterior to the globe equator.[1,2] These connective tissue sleeves are firmly anchored to each other and to the orbital walls,[1,2] and are composed of collagen and elastin stiffened by smooth muscle.[1–3] High-resolution magnetic resonance imaging (MRI) in alert subjects has demonstrated that these tissue sleeves function as pulleys for the rectus EOMs, minimizing sideslip relative to the orbit of posterior EOM paths during globe rotation and determining the effective pulling direction of each EOM.[4,5] Analysis of serial quasi-coronal (perpendicular to the long axis of the orbit) MRI images has demonstrated consistent EOM pulley positions in this plane for normal subjects.[4,5] Both large and small abnormalities of pulley locations in the coronal plane have been associated with incomitant strabismus and can mimic oblique EOM dysfunction.[6,7]

From the Departments of [1]Ophthalmology and [4]Neurology, University of California, Los Angeles; [2]Department of Ophthalmology, Kaiser Foundation Hospital, Woodland Hills; and [3]Smith-Kettlewell Eye Research Institute, San Francisco, California.

Supported by National Eye Institute grant EY-08313 (JLD, JMM). Robert A. Clark was a Rosalind W. Alcott Fellow, Heed Ophthalmic Fellow, and Giannini-Bank of America Foundation Fellow. JLD received a Research to Prevent Blindness Lew R. Wasserman merit award and is Laraine and David Gerber Professor of Ophthalmology.

Submitted for publication April 5, 2000; revised July 14, 2000; accepted July 28, 2000.

Commercial relationships policy: N.

Corresponding author: Joseph L. Demer, Jules Stein Eye Institute, UCLA, 100 Stein Plaza, Los Angeles, CA 90095-7002. jld@ucla.edu

The precise locations of EOM pulleys have important implications for ocular kinematics. Sequences of three-dimensional (3-D) rotations are noncommutative, that is, the final orientation of an object rotated about multiple (nonparallel) axes depends on the order in which the rotations are applied. A different sequence using the same rotations (i.e., both magnitude and direction of component rotations are the same) can yield a different final orientation.[8] If the oculomotor plant (globe, EOMs, and pulleys) responded to neural commands with the noncommutative behavior characteristic of a simple solid object, neural control of eye movements would have to account for this and be noncommutative as well. Thus, neural signals commanding any eye movement to a new position would have to be dependent on the initial orientation of the globe and the path taken to the final eye position. Central oculomotor control would need to be quite complex if the oculomotor plant were noncommutative. However, if EOM axes of rotation are not fixed but vary in just the right way as a function of eye position, the orbit will appear commutative to the brain. Theoretical analysis shows that suitable placement of EOM pulleys has such a "commutizing" effect and dramatically simplifies the mechanical behavior of the ocular motor plant.[9] Specifically, if the pulleys were the same distance posterior to globe center as the EOM insertions were anterior to globe center, ocular rotations would behave in an effectively commutative fashion,[9] dramatically simplifying neural control of all eye movements. With rectus pulleys in these locations (relative to the globe), the rotational axis of the EOMs would (for small angles typical of the physiological oculomotor range) rotate by half of the axis of eye rotation, thereby causing the eye to obey Listing's Law of ocular torsion.[10] Listing's Law permits many

aspects of oculomotor neural control to be specified in two, rather than three, dimensions. If the pulleys are not in the predicted locations, then oculomotor neural control must be specified in 3-D even at the level of the oculomotor plant. Thus, determination of precise pulley locations is fundamental to understanding the oculomotor system.

Because of the distributed nature of the elastic pulley tissues and their positioning in the orbit by a balance of elastic and muscular forces, the functional location of the EOM pulleys cannot be precisely defined in cadaveric material. Unlike the distinct and rigid trochlea of the superior oblique muscle, the anteroposterior length of each EOM pulley sleeve varies from 13 mm for the inferior rectus (IR) muscle to 19 mm for the medial rectus (MR) muscle, with a variable distribution of connective tissue constituents along this length.[2] In addition, individual EOM pulleys contain varying amounts of fibroelastic tissue and richly innervated smooth muscle,[2,3] and have varying mechanical coupling to the orbit and adjacent pulleys.[2,3]

The mechanical action of a pulley in stabilizing EOM path with respect to the orbit could cause an inflection in the EOM path in at least some gaze positions. Certainly, at the insertion and for some distance posteriorly up to the functional pulley, the EOM and its tendon must move to follow the insertion in the rotating eye. At the functional pulley and posteriorly, the EOM path could shift only as permitted by pulley elasticity. The inflection between the stable posterior path and moving anterior path defines the functional anteroposterior location of the pulley.

The anteroposterior pulley position has been determined in vivo by analyzing EOM paths in strabismic subjects before and after surgery to transpose the EOM insertions. The large (approximately 10 mm) surgical displacement of the EOM insertion resulted in a visible inflection between posterior and anterior EOM path segments defining the functional pulley.[11] In prior MRI studies of normal subjects, however, anterior tendons were not sufficiently resolvable for accurate determination of EOM path inflections.[4,5]

Improvements in MRI technique now permit resolution of EOM tendons anteriorly to at least the globe equator. In combination with spatial averaging across subjects, we can now describe the changes in EOM paths during gaze shifts to determine the 3-D locations of the pulleys and compare them with theoretical predictions. The present study determines pulley locations in normal subjects.

METHODS

Eleven adult volunteers were recruited by advertisement and examined to verify normal ocular motility. After obtaining written informed consent according to a protocol conforming to the Declaration of Helsinki and approved by the Human Subject Protection Committee at the University of California, Los Angeles, each subject underwent high-resolution, T1-weighted MRI using a 1.5 T General Electric Signa (Milwaukee, WI) scanner. Each subject's head was carefully stabilized in a supine position with the nose aligned to the longitudinal and the pupils to the transverse light projection references of the scanner. An array of four surface coils was deployed in phased pairs, two over each orbit, in a masklike enclosure held strapped to the face. An adjustable array of monocular, afocal, illuminated fixation targets at nine diagnostic positions of gaze was secured 2.5 cm in front of each orbit with the center target in subjective central position for each eye. Subjects were repeatedly coached to avoid unnecessary movements during scanning. Blinking was reduced by maximizing precorneal humidity using a transparent facemask and instructing subjects to avoid unnecessary blinks. Movement of the head was minimized by secure stabilization to the surface coil facemask and judicious use of padded restraints. Axial MRI images were obtained at 3.0 mm thickness using a 256 $\times$ 192 matrix over a 10-cm^2 field of view to localize placement of subsequent higher resolution quasi-coronal images perpendicular to the long axis of the orbit. Multiple contiguous quasi-coronal MRI images 2.0 mm in thickness were then obtained using a 256 $\times$ 256 matrix over an 8- or 9-cm^2 field of view, giving pixel resolutions of 313 or 352 μm, respectively. Imaging was repeated in central gaze, depression, elevation, abduction, and adduction, with data collection in some subjects limited by fatigue in maintaining fixation in eccentric gaze positions for the 3.5 minutes required. The central gaze position was determined by subjects based on self-report, and in all cases appeared reasonable to the experimenters. However, the central position does not generally correspond to the kinematic primary position, defined as an eye orientation normal to Listing's plane.

Digital MRI images were transferred to Macintosh computers (Apple Computer, Cupertino, CA), converted into 8-bit tagged image file format (TIFF) using locally developed software, and quantified using the program NIH Image (W. Rasband, National Institutes of Health; available by ftp from zippy.nimh.nih.gov or on floppy disc from NTIS, 5285 Port Royal Road, Springfield, VA 22161, part number PB95-500195GEI).

Only images free from degradation by motion or other artifacts were analyzed quantitatively. The location of each rectus EOM, and of the orbit itself, was described by a single point in each image plane using the "area centroid" function of the NIH Image program. The area centroid of a cross-section is equivalent to the center of gravity of a shape of uniform density and thickness (Fig. 1). Initially, centroid data were determined in the Cartesian coordinates of the MRI scanner. The centroids were then transformed to allow data from multiple subjects to be combined and multiple gaze angles to be compared. Left orbits were reflected to the configuration of right orbits.

It should be noted that a biomechanical analysis is concerned with the distribution of EOM forces, not EOM tissue. However, it is unknown how force is distributed across EOM cross sections. Thus, "area centroids" were calculated to describe each EOM's path, mindful that if forces are not uniformly distributed across EOM cross sections, "force centroids" might be slightly different.

Next, approximating the globe as spherical, its 3-D center was determined to subpixel resolution in scanner coordinates using curve fitting to cross-sectional images of the globe as previously described.[5,12] All rectus EOM positions were then translated to place the 3-D coordinate origin at the computed center of the globe. Our use of globe-centered translation coordinates follows from the discussion connected with Figure 8, below, showing that the kinematically important relationship is between pulley position and globe.

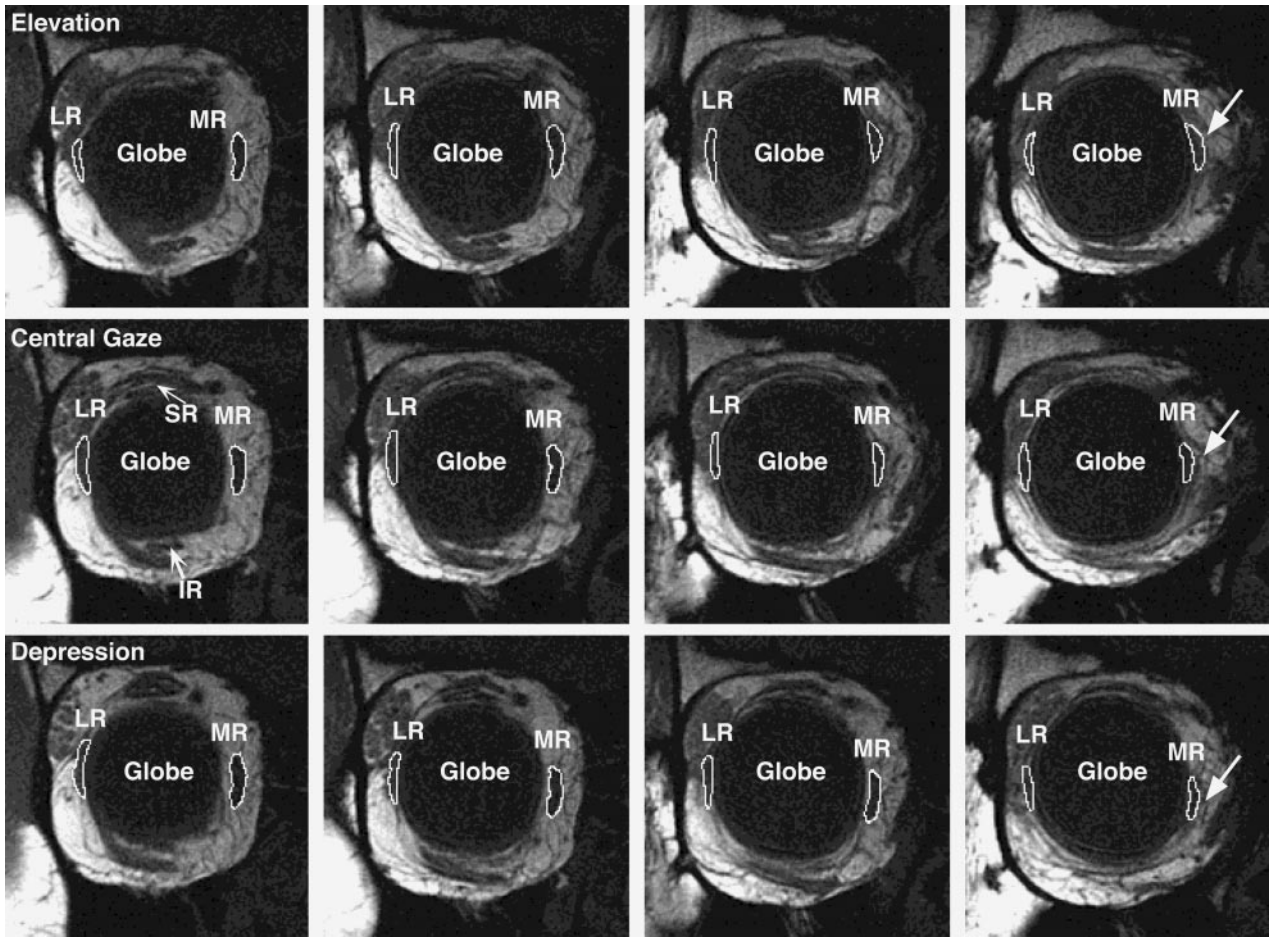

FIGURE 1. Magnetic resonance images in quasi-coronal planes near the globe equator in elevation, central gaze, and depression. Bellies and tendons of the MR and LR have been outlined in *white*. The area centroids represent geometric centers of the areas *outlined* and were used to determine EOM position. Anterior to the equator (*right side*), images show a superior shift of the MR tendon in elevation, with an inferior shift in depression. Less effect is seen for the LR tendon because the image plane perpendicular to the long axis of the orbit intersects the LR more posteriorly than the MR in the same image plane. Note the lateral position of the SR tendon compared with the IR tendon in primary position. MR, medial rectus; LR, lateral rectus; SR, superior rectus; IR, inferior rectus.

After translation, the data were rotated about the globe center using extraorbital landmarks (no suitable global referents exist). First, a horizontal rotation (yaw) was performed to align the interhemispheric fissure of the brain, which direction was taken as true anteroposterior (Fig. 2). A vertical rotation (pitch) was then performed to bring the junction of the superior ethmoid air sinus and the orbit to the standard angle of 10° elevation from true horizontal (Fig. 2). This vertical rotation was selected to be 10° because it was the mean angle required to bring the MR muscle to true horizontal in the first 20 orbits analyzed. Finally, a torsional rotation (roll) was performed to bring the interhemispheric fissure of the brain to true vertical (Fig. 2). A diagram of the rotation sequence and equations used are shown in Figure 3.[13]

After data were transformed, the scanner coordinates were scaled to millimeters based on the MRI fields of view and were then scaled to normalize each globe to the measured average diameter of 24.3 mm found on axial MRI. Displacement of the globe–optic nerve junction from its position in central gaze was used to estimate ocular rotation, as previously described.[5]

Positions of EOMs were averaged across subjects by binning data in 2-mm intervals to compute mean anteroposterior, horizontal, and vertical coordinates. To determine inflections in horizontal EOM paths in secondary vertical gaze positions, we analyzed only those orbits for which there were complete image sets in central gaze, elevation, and depression. Likewise, to determine inflections in vertical EOM paths in secondary horizontal gaze positions, we analyzed only orbits for which there were complete image sets in central gaze, abduction, and adduction. Area centroids of EOMs could not be discerned at all anteroposterior positions in all subjects, but each average EOM centroid was determined at 2-mm intervals based on data from five or more orbits.

Inflections were determined objectively using piecewise linear regression on geometrically corrected EOM mean area centroid coordinates. The area centroid data representing the length of each EOM was systematically divided into all possible sets of contiguous anterior and posterior parts by systematically varying the dividing point in increments corresponding to the 2-mm bins. Linear regressions and corresponding coefficients of variation (R^2) were then computed separately for

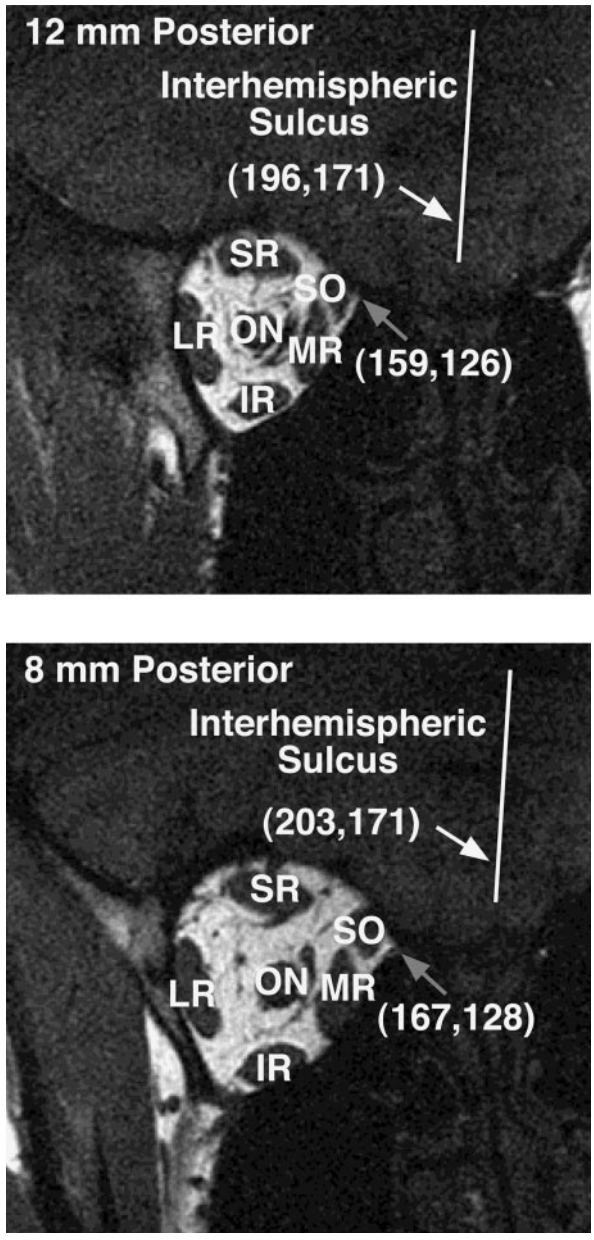

FIGURE 2. Magnetic resonance images in quasi-coronal planes 12 and 8 mm posterior to the globe-optic nerve junction. The craniotopic landmarks used to measure 3-D rotation angles were the interhemispheric sulcus (*white arrows*) and the junction of the superior ethmoid air sinus and the orbit (*gray arrows*). The first rotation angle (yaw) was determined by the horizontal displacement of the interhemispheric sulcus from the posterior orbit moving anteriorly, in this case as 7 pixels {203 − 196} or, converting to mm, a 2.2-mm medial displacement over a 4.0-mm anterior path. The yaw rotation angle was ($-\tan^{-1}[2.2/4.0]$), or −28° to rotate the interhemispheric sulcus into a true anteroposterior direction (see Fig. 3 for definition of sense of coordinate system). The second rotation angle (pitch) was determined by the vertical displacement of the junction of the superior ethmoid air sinus and the orbit, in this case as 2 pixels {128 − 126} or, converting to mm, a 0.6-mm superior displacement over 4 mm. The pitch correction was ($10° - \tan^{-1}[0.6/4]$), or 1°. The final rotation angle (roll) was the angle needed to rotate the interhemispheric sulcus to true vertical, in this case 2°. SO, superior oblique.

each of the two corresponding parts for each dividing point, until all possible contiguous variations of anterior and posterior data points were analyzed. The best estimate of the inflection point for each EOM was taken to be the intersection of the two regressions having the greatest summed coefficients of variation. This procedure avoided subjective bias in determination of inflection points, although the results were consistent with the subjective appearance of the data.

Finally, translation of the globe with respect to the bony orbit was estimated by calculating the area centroid of the orbit at the level of the globe–optic nerve junction in the previously defined oculocentric coordinate system, for all gaze positions. Movement of the orbital area centroid actually reflects translation of the globe center.

RESULTS

The 11 normal subjects ranged in age from 21 to 33 years (average, 28.5 years). Based on the change in position of the globe–optic nerve junction, average elevation (21.8°) and depression (21.9°) were nearly identical, but there was a trend toward greater adduction (34.4°) than abduction (20.2°, $P = 0.10$).

It was possible to determine area centroids by outlining EOM cross sections throughout their posterior extents and usually as far anteriorly as the globe equator for the IR, lateral rectus (LR), and superior rectus (SR). Because MRI images

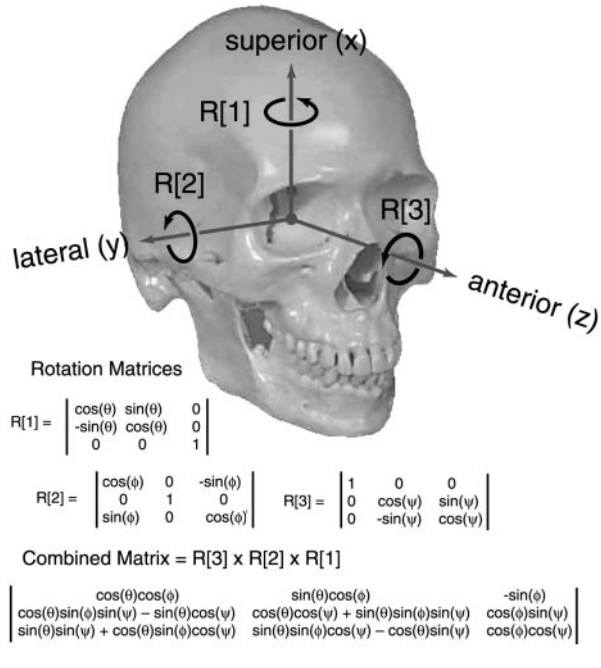

FIGURE 3. Sequence of rotations and rotation matrices. After the EOM area centroid data were translated using the Cartesian coordinate system X, Y, Z with the positive sense indicated to place the origin at globe center, three rotational corrections were applied to the data in the sequence indicated. The first rotation R[1] (yaw) was a horizontal rotation of $\theta°$ around the vertical axis labeled (X). The second rotation R[2] (pitch) was a vertical rotation of $\phi°$ around the horizontal axis labeled (Y). The third rotation R[3] (roll) was a torsional rotation of $\psi°$ around the anteroposterior axis labeled (Z).

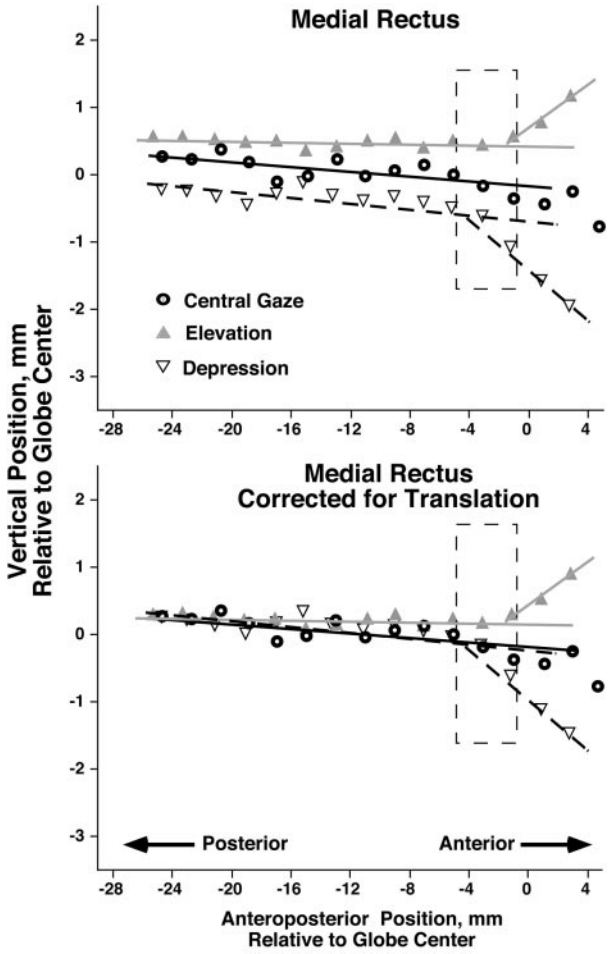

FIGURE 4. Average vertical area centroid positions of the medial rectus (MR) muscle along the anteroposterior orbital axis, with zero referenced to globe center. *Top*: The MR path uncorrected for globe translation with changes of gaze (oculocentric), where the posterior MR path apparently sideslipped approximately 0.5 mm in the direction of gaze. *Bottom*: The corrected MR path for this translation (orbitocentric), greatly reducing the apparent sideslip of the posterior MR path relative to the orbit. In both graphs, optimum piecewise linear regression lines on the posterior and anterior EOM paths, respectively, show discrete MR path inflection superiorly in elevation and inferiorly in depression. This inflection in MR path both indicates the pulley effect and localizes its anteroposterior pulley position. The experimental uncertainty in anteroposterior location of the MR pulley is delineated by the width of the *dotted rectangle*, ± one MRI plane thickness.

were obtained perpendicular to the long axis of the orbit, images apparently bisecting the globe equator actually intersect the MR further anterior. This geometry and the presence of high contrast in surrounding orbital tissues consistently enabled clear definition of area centroids for the MR anterior to the globe equator, as seen in the right column of Figure 1. Area centroids of the cross sections of EOMs in the posterior orbit provide the best estimate of EOM path, although they may not precisely reflect force centroids, as we have explained. Area centroids of EOM cross sections anterior to the pulleys should faithfully represent force centroids.

Area centroids of each of the four rectus EOMs were averaged across subjects. Because of the care used in positioning subjects during imaging, most of the rotation angles were similar among patients, yielding final data clustered according to original MRI image depth. The anteroposterior, superior, and lateral area centroid coordinates were averaged for each data cluster to yield an average single area centroid in all three dimensions. The SEM for every determination of each EOM area centroid was less than 0.5 mm (range, 0.20–0.45 mm). The average path of each EOM was fit by a two-segment linear regression. For all EOMs, there were in secondary gaze positions differences in the slopes of the two regressions indicating distinct path inflections. The inflections were located 3 to 9 mm posterior to the globe equator (Figs. 4 through 7).

The globe itself showed characteristic translations with gaze shifts (Table 1), as indicated by apparent displacement of the area centroid of the orbit in the oculocentric coordinate system. Data for each rectus EOM are presented graphically two ways to demonstrate the effect of globe translation on EOM position. First, data relative to globe center are presented for each EOM, showing the relative stability of all posterior EOM paths relative to the globe. The data are again depicted after subtractive correction for globe translation, to show the stability of the posterior EOMs relative to the orbit. This orbitocentric depiction, corrected for globe translation, allows direct comparison of posterior EOM stability with previous studies that referenced EOM positions only to the bony orbit.[5,7,11]

Figure 4 (top) shows oculocentric vertical MR position in central gaze, elevation, and depression. If no pulley had existed, the MR path would have followed an approximately straight line from the orbital apex to the vertically displaced MR insertion. Instead, with respect to the center of the globe (Fig. 4, top), there was a small (<1 mm) shift in posterior MR position toward the direction of gaze. Anteriorly, there was a large deflection of the MR path in the direction of gaze beginning approximately 3 mm posterior to the center of the globe. The MR path abruptly changed within an interval of 2 mm, the thickness of one MRI image. This inflection in MR path both confirms the existence of an effective pulley and defines its functional location.

Figure 4 (bottom) is an orbitocentric depiction of the path of the MR, showing stability of the posterior path relative to the orbit. Nearly all the oculocentric vertical displacement of the posterior MR path during changes of gaze can be attributed to inferior globe translation on elevation and the superior globe translation on depression.

The inflections in MR path for elevation and depression, as determined by piecewise linear regression for anterior and posterior MR area centroids, occurred at slightly different anteroposterior positions. This difference is less than ±2 mm, the thickness of one MRI image. The average primary position MR

TABLE 1. Globe Translation Relative to the Orbit in Secondary Gaze Positions Compared with Central Gaze

	Lateral (mm)	Superior (mm)
Elevation	−0.1	−0.3
Depression	−0.4	0.5
Abduction	−0.2	0.1
Adduction	−0.7	0.0

Positive changes are defined as superior and lateral.

TABLE 2. Normal Rectus Pulley Positions Relative to Globe Center

	Anterior	Lateral	Superior
Medial rectus	−3 ± 2	−14.2 ± 0.2	−0.3 ± 0.3
Lateral rectus	−9 ± 2	10.1 ± 0.1	−0.3 ± 0.2
Superior rectus	−7 ± 2	−1.7 ± 0.3	11.8 ± 0.2
Inferior rectus	−6 ± 2	−4.3 ± 0.2	−12.9 ± 0.1

Positive coordinates are defined as anterior, superior, and lateral relative to globe center. For anteroposterior position, the error bars represent one MRI image plane thickness (2 mm). For lateral and superior position, the error bars represent 95% confidence intervals for the lateral and superior coordinates of primary position for all subjects at that anteroposterior EOM position.

path at the midpoint between the inflections was 3 mm posterior, 14.0 mm medial, and 0.3 mm inferior to globe center (Table 2).

Figure 5 (bottom) is an orbitocentric depiction of the vertical position of the LR in central gaze, elevation, and depression. Inferior displacement of the posterior LR path occurred in elevation with superior displacement in depression. This seemingly paradoxical movement has been noted previously and attributed to coupling of the LR to the superior rectus (SR) through the lateral levator aponeurosis.[5] For the LR, however, this paradoxical movement nearly negated the displacement of the posterior LR path relative to globe center because it mirrored globe translation. This negation of LR path movement is shown in the oculocentric depiction (Fig. 5, top) by the relative stability of the posterior LR path with respect to the center of the globe.

As for the MR, the inflections in LR path on elevation and depression were not at identical anteroposterior locations. Again, this difference was less than plus or minus one MRI image plane thickness of 2 mm. Average position of the LR pulley was 9 mm posterior, 10.1 mm lateral, and 0.3 mm inferior to globe center (Table 2).

Figure 6 (top) is an oculocentric depiction of the horizontal path of the SR in central gaze, abduction, and adduction. To illustrate the inflections more clearly, all data has been transformed by rotating the oblique SR path from medial to lateral in central gaze to horizontal on the graph, while retaining the true anteroposterior position of all data points. (Had this not been done, the posterior SR path in all gaze positions would have been markedly oblique, and the graphs would have been difficult to visualize.) There was very little change in the posterior path of the SR with gaze shifts in either oculocentric or orbitocentric depictions (Fig. 6, bottom). The posterior path of the SR belly was consistently sinuous, probably reflecting variation in cross-sectional shape because of cross-section thickening at the fusion of the levator palpebrae superioris with the SR in midorbit.

Again, inflections in SR path on adduction and abduction were not at identical anteroposterior positions. Again, this difference was less than plus or minus one MRI image thickness of 2 mm. Average position of the SR pulley was 7 mm posterior, 1.7 mm medial, and 11.8 mm superior to globe center (Table 2).

Figure 7 (top) is an oculocentric depiction of the horizontal position of the IR relative to globe center in central gaze, abduction, and adduction. As for the SR, all data has been transformed to rotate the oblique posterior IR path from medial to lateral in central gaze so that it appears horizontal on the graph, while retaining the true anteroposterior position of all the data points. In an oculocentric reference, the posterior path of the IR was displaced laterally in adduction and medially in adduction (Fig. 7, top). Subtracting globe translation to obtain an orbitocentric reference, the only substantial posterior IR sideslip was medial displacement on abduction (Fig. 7, bottom). The posterior path of the IR belly was consistently sinuous, probably reflecting variations in cross-sectional shape.

The inflections in IR path on abduction and adduction differed by almost exactly one MRI image thickness, 2 mm.

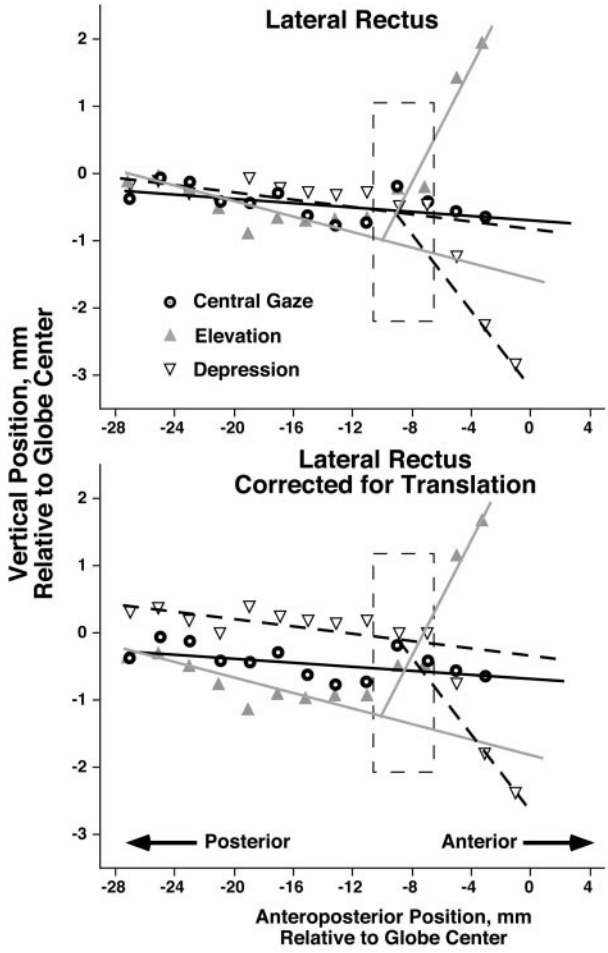

FIGURE 5. Average vertical area centroid positions of the LR muscle along the anteroposterior orbital axis, relative to globe center. *Top*: The LR path uncorrected for globe translation (oculocentric), where the posterior LR path shows little sideslip. *Bottom*: When globe translation is subtracted (orbitocentric), the posterior LR path displaced superiorly in depression and inferiorly in elevation by approximately 0.5 mm. In this case, globe displacement was in the same direction as LR sideslip with changes of gaze, effectively increasing the relative stability of the posterior path of the LR relative to globe center. In both graphs, optimum piecewise linear regression lines on the posterior and anterior EOM paths, respectively, show discrete LR path inflection superiorly in elevation and inferiorly in depression beginning approximately 9 mm posterior to globe center. This inflection in LR path both indicates the pulley effect and localizes its anteroposterior pulley position. The experimental uncertainty in location of the LR pulley is delineated by the width of the *dotted rectangle*, ± one MRI plane thickness.

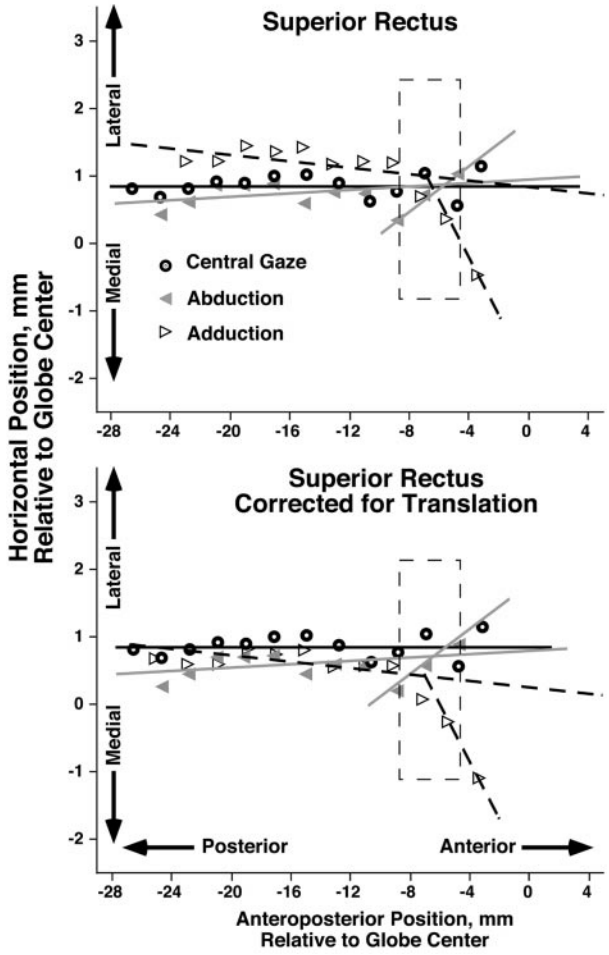

Figure 6. Average horizontal area centroid positions of the SR muscle along the anteroposterior orbital axis, relative to globe center. To show inflections in SR paths more clearly, the data has been transposed to make the best-fit linear regression of central gaze parallel to the abscissa. Although the data has been transposed, the true anteroposterior coordinates of each of the points have been maintained to allow interpretation of the data in the coordinate system used in Figures 4 and 5. *Top*: The SR path uncorrected for globe translation (oculocentric), where only a small, approximately 0.5-mm lateral displacement of the posterior path of the SR occurred during adduction. *Bottom*: When globe displacement has been subtracted (orbitocentric), very little sideslip of the posterior SR path occurred. In both graphs, optimum piecewise linear regression lines on the posterior and anterior EOM paths, respectively, show discrete SR path inflection laterally in abduction and medially in adduction beginning approximately 7 mm posterior to globe center. This inflection in SR path both indicates the pulley effect and localizes its anteroposterior position. The experimental uncertainty in location of the SR pulley is delineated by the width of the *dotted rectangle*, ± one MRI plane thickness.

Interpolating between the adjacent points in central gaze, the average position of the IR pulley was 6 mm posterior, 4.3 mm medial, and 12.9 mm inferior to globe center (Table 2).

Discussion

Correlation of high-resolution MRI with modern orbital histology has provided valuable new insights into the role of orbital mechanics in ocular kinematics. Theories of EOM behavior have evolved from the "shortest path" hypothesis, where EOM bellies were assumed to have complete freedom in the orbit to assume positions minimizing mechanical tension,[14] to the "permitted sideslip" hypothesis, where musculo-global constraints allowed limited EOM path displacements,[15–17] to the concept of musculo-orbital constraints on EOM paths. The most recent

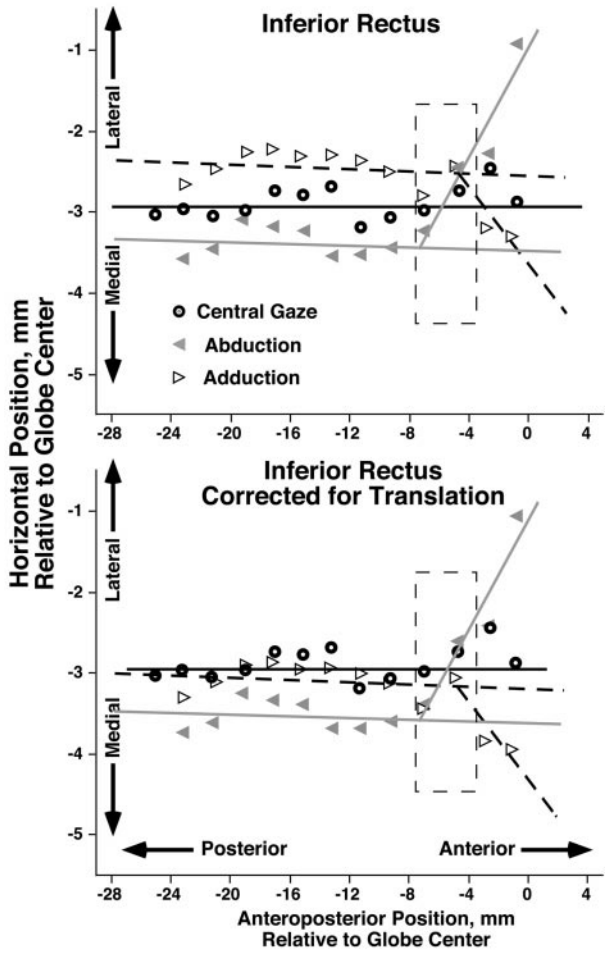

Figure 7. Average horizontal area centroid positions of the IR muscle along the anteroposterior orbital axis, relative to globe center. To show inflections in IR paths more clearly, the data has been transposed to make the best-fit linear regression of central gaze parallel to the abscissa. Although the data has been transposed, the true anteroposterior coordinates of each of the points have been maintained to allow interpretation of the data in the coordinate system used in Figures 4 through 6. *Top*: The IR path uncorrected for globe translation (oculocentric), where small, 0.5-mm shifts in IR posterior path occurred opposite the direction of gaze (i.e., lateral displacement on adduction and medial displacement on abduction). *Bottom*: When globe displacement is subtracted (orbitocentric), little sideslip of the posterior path of the IR occurred in adduction, but there was nonetheless approximately 0.5-mm medial displacement during abduction. In both graphs, optimum piecewise linear regression lines on the posterior and anterior EOM paths, respectively, show discrete IR path inflection laterally in abduction and medially in adduction beginning approximately 6 mm posterior to globe center. This inflection in IR path both indicates the pulley effect and localizes its anteroposterior pulley position. The experimental uncertainty in location of the IR pulley is delineated by the width of the *dotted rectangle*, ± one MRI plane thickness.

evidence implicates the midorbital region, where histology has defined connective tissue structures that restrain EOM sideslip and function as pulleys for the rectus EOMs.[2] Previous studies using high-resolution MRI have confirmed that the posterior EOM bellies, behind the posterior border of the globe, are resistant to sideslip both during normal gaze changes as well as after surgical transposition.[4,5,11,18]

The present study determined rectus EOM paths from area centroids of EOMs in quasi-coronal MRI image planes. As an estimate of force centroids, this approach assumes a uniform distribution of oculorotatory forces over an EOM's cross section. Rectus EOMs, however, consist of two layers, only one of which directly rotates the eye: the global layer inserts in the globe, whereas the orbital layer inserts in the corresponding pulley.[19] The orbital layer contains approximately 40% of total EOM fibers and is typically C-shaped, surrounding the global layer except on the global surface.[20] Although we could not distinguish the two layers in our MRI data, it is doubtful that the inclusion of orbital fibers significantly influenced the estimates of pulley positions because the orbital layer is not present in anterior sections, which are critical to our estimates of pulley position. In the posterior orbit, the sinuous course of the rectus EOMs (Figs. 4 to 7) is probably related to variation in orbital fiber contractile state and in the midorbital region of the SR with fusion with the levator palpebrae superioris. Deep in the orbit at the motor nerve entry zone, rectus EOMs also thicken, unrelated to EOM force, as up to half the cross section is comprised of luxuriant nerve fibers.[21]

On the basis of the elongated nature of the pulley sleeves observed histologically, one might have imagined that their mechanical behavior would be like that of smoothly bending elastic tubes. Instead, the data show that the EOM path inflection to be sharp in most cases. This finding is consistent with the sharp inflection in EOM paths seen after surgical transposition in a prior MRI study quantifying the anteroposterior location of postsurgical EOM pulleys.[11] Thus, it is reasonable in modeling to describe each pulley's functional location as a point.

This study also assumes that all orbits can be transformed into the same anatomic configuration using consistent extraorbital landmarks. Prior studies referenced EOM position with respect to the center of the bony orbit, minimizing the effect of misalignments in head position during scanning.[5,7,11] However, with orbital referents the data are not related to the eye itself in a meaningful way. The positions of the EOM pulleys with respect to the eye, not the orbit, are the determinants of kinematic behavior, and their true anatomic positions are required for accurate biomechanical modeling of ocular motility.

The landmarks chosen for rotational alignment of the orbits represent stereotypic cranial features seen in an 8- or 9-cm, field of view MRI centered on the orbit. These landmarks proved reliable in the 11 normal subjects analyzed but might not be as reliable for analysis of subjects with significant cranial dysmorphism. Hemifacial asymmetry with obvious distortion of the interhemispheric fissure of the brain, for example, may render that anatomic landmark useless and prevent an accurate correction of the horizontal and torsional components of head position. The effect of measurements errors of the different rotational angles is minimized, however, by using the globe center as the origin of the coordinate system. By simple geometry, even large cranial angular positioning errors lead to small linear shifts in EOM positions close to the coordinate system center, the region in which the EOM pulleys were found in this study.

A third assumption is that the position of EOM deflection defines the pulley position. This assumption was also explicit in prior MRI studies of the pulleys,[5,7] because even high-resolution MRI was not sufficient to delineate the EOM pulley tissue itself. The distinction between EOM position and pulley tissue is not relevant to this study, however, because the functional pulley position is defined mechanically by the inflection in EOM path, irrespective of the pulley connective tissue components. Although EOM position alone is sufficient to define both the pulley effect and the pulley position, further refinements in MRI technique have now directly imaged pulley constituents at the EOM path inflections.[10]

A fourth assumption of this study is that pulley positions were not affected significantly by unintended gaze eccentricities (i.e., horizontal eccentricity in a comparison of vertical gaze positions, and vice versa). Reexamination of EOM anatomy has revealed that the orbital layer of each rectus EOM inserts directly on the pulley tissue, whereas the global layer continues anteriorly to insert on the sclera.[10,19,21] This finding, as well as MRI in the plane of contracting EOMs, suggests the active pulley hypothesis: that anteroposterior pulley locations are dynamically regulated by the action of the orbital layers to control ocular kinematics in tertiary gaze positions.[10,19,21] The insertion of the orbital layer appears suited to shift the pulley posteriorly during EOM contraction and anteriorly during EOM relaxation.[10,19,21] The possible effect of an actively generated shift in anteroposterior pulley position was avoided by measuring the EOM paths only in central and secondary gaze positions. In this study, a slight bias toward abduction during nominal central target fixation resulted in more average adduction than abduction (34.4 vs. 20.2°). Although not statistically significant, mechanically this bias might have resulted in relative anterior displacement of the relaxed MR pulley and posterior displacement of the tightened LR pulley compared with true central gaze. Examination of EOM path inflections in tertiary gaze positions (e.g., adducted elevation and depression vs. abducted elevation and depression) would test the prediction that EOM pulley positions vary with gaze and EOM contractility. Such a study would require further technical improvements in MRI resolution of anterior EOM tendons, possibly achievable using a paramagnetic contrast agent.[22]

Listing's Law states that, when the head is upright and stationary, all possible axes of ocular rotation lie in a single plane. Kinematic "primary position" is the direction normal to Listing's plane[23] and is in general different from our arbitrarily selected "central gaze" position. To implement a linear oculomotor plant with commutative properties and simplify implementation of Listing's Law, pulleys were predicted to be located as far posterior to globe center as the insertions of their respective EOMs are to anterior to globe center.[9,10,19] In particular, these distances must be equal relative to Listing's plane passing through the center of the globe. Although Listing's plane has little or no vertical tilt relative to the frontoparallel, the mean yaw tilt of Listing's plane is 11° temporal, with a 95% confidence interval of 7 to 25°.[24] Considering the variation in location of the insertions of the rectus EOMs relative to the limbus in a normal eye,[25] this corresponds to pulley locations 5 to 7 mm posterior to Listing's plane. The pulley positions

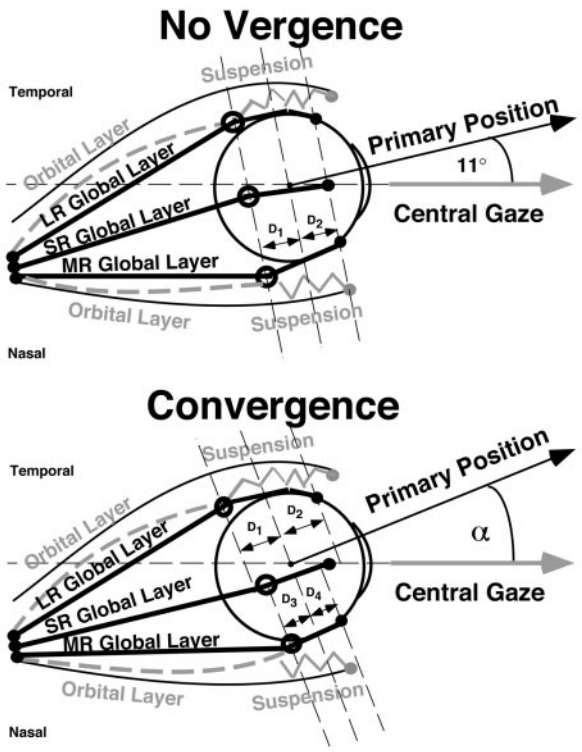

FIGURE 8. Scale diagram of LR, MR, and SR pulleys relative to their respective EOMs and the globe in the nonvergence state (*top*), and in convergence of the fellow eye to a target aligned to the eye illustrated. *Top*: *Three dotted parallel reference lines* are drawn through the horizontal rectus insertions, globe center, and the pulleys. Relative to these reference lines, distance D_1 from pulleys to globe center is equal to distance D_2 from globe center to all three rectus insertions, as required to implement Listing's half angle rule that the axis of rotation of the eye shift by half the shift in eye orientation. The *perpendicular* to these reference lines is perpendicular to Listing's plane and thus defines kinematic primary position. The kinematic primary position inferred from this scale diagram is 11° temporal to central gaze, matching the reported mean orientation of primary position in normal subjects. [25] The *bottom* diagram shows how pulley reconfiguration in convergence could produce a temporal shift in kinematic primary position to angle α, associated with an anterior shift in the MR pulley, posterior shift in the LR pulley, and medial and anterior shift in the SR (and IR, not shown) pulleys. In convergence, $D_1 = D_2 > D_3 = D_4$. Posterior pulley shifts could be produced by contraction of the orbital layers of the respective rectus EOMs against the elastic suspensions of the respective pulleys from the anterior orbit; nasal shift of the vertical rectus pulleys in convergence could be produced by contraction of the peribulbar smooth muscle (not shown).

measured here for the vertical rectus EOMs fall roughly within that predicted range, supporting the theoretical requirements of the linear oculomotor plant. Figure 8 (top) is a top view, scaled diagram of the measured positions of the LR, MR, and SR pulleys in central gaze without vergence. If primary position is assumed to be 11° temporal to central gaze, then the predicted requirements of a linear oculomotor plant are satisfied to within experimental error.

Although the temporal tilting of Listing's plane may suffice to account for the observed anterior position of the MR pulley, there are theoretical grounds to anticipate that the effect might be further magnified by convergence. During convergence, the Listing's planes for the two eyes are reported by various authors to rotate temporally by between 16% and 100% of the vergence angle, but most commonly 25%,[26] corresponding to the relative excyclotorsion in depression and incyclotorsion in elevation[27,28] necessary to maintain alignment of corresponding retinal meridia during near viewing. Thus, during binocular viewing of near and far targets aligned on one eye, the Listing plane for that unmoving eye nevertheless tilts in association with the vergence movement of the other eye.[29] In the present experiment, convergence to the near target may have occurred in some subjects despite the nonaccommodative target's monocular presentation aligned to the scanned eye. Figure 8 (bottom) depicts a situation in which a near target is aligned to the diagrammed eye, with the entire vergence angle generated by the fellow eye (not shown). In such a convergent situation, pulleys could implement a linear plant with a temporal shift of Listing's primary position by anterior displacement of the MR pulley, nasal and anterior displacement of the SR pulley, and posterior displacement of the LR pulley. The peribulbar smooth muscle is anatomically situated to accomplish much of the required pulley displacements.[19] Note that in the convergent case where Listing's primary position is oriented temporally from central gaze to angle α, the distance D_1 from the LR pulley to globe center can be equal to the distance D_2 from globe center to the LR insertion, and distance D_3 from the MR pulley to globe center can be equal to distance D_4 from globe center to the MR insertion, although $D_1 > D_3$. Suitable MRI studies during controlled convergence could test this hypothesis.

The present study found the normal pulley positions to be slightly more anterior than had been previously shown in postsurgical patients,[11] where EOM path inflections occurred between 3 and 6 mm anterior to the globe–optic nerve junction along the long axis of the orbit. There are three potential explanations for the difference in anteroposterior position. First, surgical dissection weakens the anterior pulley slings, allowing them to retract posteriorly. Second, transposition surgery moves the EOM insertion approximately 10 mm from its normal location. The average change in EOM insertion during changes of gaze, calculated assuming normal anatomic insertions[25] and globe geometry, varied from a minimum of a 1.8 mm temporal shift in the SR insertion during abduction to a maximum of 4.1 mm nasal shift of the IR insertion during adduction. The nonphysiologically larger changes in EOM insertions produced by transposition surgery may stretch the anterior pulley tissue more than normal, moving effective pulley position posterior into denser connective tissue. Finally, the study on the effect of transposition surgery on EOM paths did not relate the EOM paths to any standard anatomic coordinate system, presenting the data referenced to the center of the bony orbit.[11] along the long axis of the orbit. The true anatomic anteroposterior location of the EOM pulleys after transposition surgery remains to be accurately defined. Direct surgical manipulations of the pulleys for the treatment of strabismus may be possible even without manipulations of the scleral insertions, and deserve consideration by surgical innovators.

An unexpected finding is the asymmetry in horizontal location of the vertical rectus pulleys. The MR and LR pulleys were at the same vertical level, 0.3 mm inferior to globe center. Conversely, the SR pulley was only 1.7 mm nasal and 7 mm

posterior to globe center, whereas the IR pulley was 4.3 mm nasal and 6 mm posterior to globe center. Even casual analysis of the MRI planes (Fig. 1) demonstrates a substantial lateral displacement of the SR belly compared with the IR belly in anterior image planes. Projecting the observed lateral displacement of the SR anteriorly in the orbit toward its insertion would result in a SR insertion 4.3 mm lateral to true vertical on the globe, compared with an IR insertion 0.3 mm nasal to true vertical. Such an arrangement would not permit a direct balancing of vertical forces between the SR and IR, and, in fact, is not observed in anatomic analysis of the EOM insertions.[25] A more reasonable hypothesis is that the SR path deflects into a nearly true anteroposterior path as the EOM belly passes through the pulley toward its insertion, permitting the SR insertion to align vertically with the IR insertion. The relative posterior location of the more laterally located SR pulley is consistent with a temporal tilt of Listing's plane (Fig. 8).

Globe translation during gaze shifts represents an important variable to control when assessing posterior EOM stability. Although the magnitude of globe displacement is small, averaging much less than 1 mm, it is nonetheless significant because it alters the relative origins of the pulleys that are themselves located close to the center of the globe. For example, the 0.8-mm shift in globe center relative to the orbital-fixed MR pulley alters the torsional action of the MR by approximately 3.3° from elevation to depression. Globe translation comprises the greatest part of relative posterior EOM sideslip for all the EOMs except the LR. For the LR, globe translation is in the same direction as LR sideslip, decreasing the relative sideslip of the LR with respect to globe center. The cause of the globe translation is uncertain. It may be related to the action of the oblique EOMs, with the posteriorly inserted superior oblique translating the globe superiorly in depression and the inferior oblique translating the globe inferiorly in depression.

The magnitude and direction of posterior EOM path displacements, after correction for globe translation, is remarkably similar to our previous study of EOM path stability relative to the bony orbit.[5] In both the present study and the earlier study, the MR, SR, and IR posterior paths showed little sideslip during changes of gaze perpendicular to the their directions of action. Both studies showed superior displacement of the posterior path of the LR during depression and inferior displacement during elevation.[5] We had previously interpreted the gaze-related shift of the LR path to its coupling to the SR through the lateral levator aponeurosis.[5] Given the similarity in magnitude and direction between the LR path and globe displacement, movement of the LR may instead be related to coupling between the LR pulley and the globe, and to a less rigid coupling of the LR pulley to the bony orbital wall. The postulated coupling of the LR pulley to the globe need not be direct, but might be distributed through broad contact with posterior Tenon's fascia.

In conclusion, analysis of normal rectus EOM paths confirms the existence of functionally discrete pulleys whose 3-D locations are consistent with the theoretical requirements of a linear oculomotor plant, one that has commutative properties and thus facilitates neural control conforming to Listing's law. The EOM pulleys may simplify neural control of eye movements by implementing a linear ocular motor plant for which commands for 3-D eye velocity are effectively independent of eye position. Normal pulley positions are anterior to those observed after surgical transposition of the EOM insertions, suggesting that pulley positions might be therapeutically altered for the treatment of strabismus. Direct surgical manipulations of the pulleys might even be possible even without manipulations of the scleral insertions. Systematic translation of the globe occurs in secondary gaze positions that alters the locations of specific EOM pulleys with respect to the globe center. Exaggeration of globe translation due to pathology of orbital connective tissues could potentially produce marked abnormalities in EOM action, and this mechanism might be added to pulley heterotopy[7] as a potential cause of strabismus.

Acknowledgment

Lance M. Optican provided a helpful critique of the manuscript.

References

1. Koornneef L. New insights in the human orbital connective tissue. Result of a new anatomical approach. *Arch Ophthalmol.* 1977;95: 1269–1273.
2. Demer JL, Miller JM, Poukens V, Vinters HV, Glasgow BJ. Evidence for fibromuscular pulleys of the recti extraocular muscles. *Invest Ophthalmol Vis Sci.* 1995;36:1125–1136.
3. Demer JL, Poukens V, Miller JM, Micevych P. Innervation of extraocular pulley smooth muscle in monkeys and humans. *Invest Ophthalmol Vis Sci.* 1997;38:1774–1785.
4. Miller JM. Functional anatomy of normal human rectus muscles. *Vision Res.* 1989;29:223–240.
5. Clark RA, Miller JM, Demer JL. Location and stability of rectus muscle pulleys: muscle paths as a function of gaze. *Invest Ophthalmol Vis Sci.* 1997;38:227–240.
6. Demer JL, Miller JM, Poukens V. Surgical implications of the rectus extraocular muscle pulleys. *J Pediatr Ophthalmol Strabismus.* 1996;33:208–218.
7. Clark RA, Miller JM, Rosenbaum AL, Demer JL. Heterotopic rectus muscle pulleys or oblique muscle dysfunction? *J AAPOS.* 1998;2: 17–25.
8. Haslwanter T. Mathematics of 3-dimensional eye rotations. *Vision Res.* 1995;35:1727–1739.
9. Quaia C, Optican LM. Commutative saccadic generator is sufficient to control a 3-D ocular plant with pulleys. *J Neurophysiol.* 1998; 79:3197–3215.
10. Demer JL. Orbital connective tissues in binocular alignment and strabismus. In: Lennerstrand G, Ygge J, eds. *Advances in Strabismus Research: Basic and Clinical Aspects.* London: Portland Press; (In press).
11. Clark RA, Rosenbaum AL, Demer JL. Magnetic resonance imaging after surgical transposition defines the anteroposterior location of the rectus muscle pulleys. *J AAPOS.* 1999;3:9–14.
12. Mason TE, Hazard CT. *Brief Analytic Geometry.* Boston: Ginn and Company; 1935:72–73.
13. Pipes LA. *Matrix Methods for Engineering.* Englewood Cliffs, NJ: Prentice-Hall; 1963:172–174.
14. Krewson WE. The action of the extraocular muscles: a method of vector analysis with computations. *Trans Am Ophthalmol Soc.* 1950;48:443–486.
15. Robinson DA. A quantitative analysis of extraocular muscle cooperation and squint. *Invest Ophthalmol Vis Sci.* 1975;14:801–825.
16. Miller JM, Robinson DA. A model of the mechanics of binocular alignment. *Comput Biomed Res.* 1984;17:436–470.
17. Miller JM, Robins D. Extraocular muscle sideslip and orbital geometry in monkeys. *Vision Res.* 1987;27:381–392.
18. Miller JM, Demer JL, Rosenbaum AL. Effect of transposition surgery on rectus muscle paths by magnetic resonance imaging. *Ophthalmology.* 1993;100:475–487.
19. Demer JL, Oh SY, Poukens V. Evidence for active control of rectus extraocular muscle pulleys. *Invest Ophthalmol Vis Sci.* 2000;41: 1280–1290.

20. Oh SY, Poukens V, Demer JL. Quantitative analysis of rectus extraocular muscle layers in monkey and human. Abstracts of 26th Annual Meeting of the American Association for Pediatric Ophthalmology and Strabismus, San Diego, CA; 2000. p. 22.
21. Demer JL. Extraocular muscles. In: Jaeger EA, Tasman PR, eds. *Clinical Ophthalmology.* Section 1, Chapter 1. Philadelphia: Lippincott, Williams, and Wilkins; 2000:1–23.
22. Oh S, Poukens V, Demer JL. Quantitative analysis of vascularity in human rectus extraocular muscle layers [ARVO Abstract]. *Invest Ophthalmol Vis Sci.* 2000;41(4):**S**417. Abstract nr 2203.
23. Haustein W. Considerations on Listing's Law and the primary position by means of a matrix description of eye position control. *Biol Cybern.* 1989;60:411–420.
24. Haslwanter T, Curthoys IS, Black R, Topple A. Orientation of Listing's plane in normals and in patients with unilateral vestibular deafferentation. *Exp Brain Res.* 1994;101:525–528.
25. Apt L, Call NB. An anatomical reevaluation of rectus muscle insertions. *Trans Am Ophthalmol Soc.* 1980;78:365–375.
26. Tweed D. Visual-motor optimization in binocular control. *Vis Res.* 1997;37:1939–1951.
27. van Rijn LJ, van den Berg AV. Binocular eye orientation during fixations: Lising's law extended to include eye vergence. *Vision Res.* 1993;33:691–708.
28. Somani RAB, Desouze JFX, Tweed D, Vilis T. Visual test of Listing's law during vergence. *Vision Res.* 1998;38:911–923.
29. Steffen H, Walker MF, Zee DS. Rotation of Listing's plane with convergence: independence from eye position. Invest Ophthalmol Vis Sci 2000;41:715–721.